Available online at www.sciencedirect.com
ScienceDirect
Journal of Power Sources 163 (2007) 997–1002
JOURNAL OF POWER SOURCES
www.elsevier.com/locate/jpowsour

Short communication

Understanding the effect of TiO_2, VCl_3, and $HfCl_4$ on hydrogen desorption/absorption of $NaAlH_4$

Yindee Suttisawat [a], Visara Jannatisin [a], Pramoch Rangsunvigit [a,*], Boonyarach Kitiyanan [a], Nongnuj Muangsin [b], Santi Kulprathipanja [c]

[a] *Petroleum and Petrochemical College, Chulalongkorn University, Bangkok 10330, Thailand*
[b] *Department of Chemistry, Chulalongkorn University, Bangkok 10330, Thailand*
[c] *UOP LLC, 50 East Algonquin Road, Des Plaines, IL 60017, USA*

Received 8 June 2006; received in revised form 26 September 2006; accepted 26 September 2006
Available online 15 November 2006

Abstract

The main objective of this work was to investigate the different effects of transition metals (TiO_2, VCl_3, $HfCl_4$) on the hydrogen desorption/absorption of $NaAlH_4$. The $HfCl_4$ doped $NaAlH_4$ showed the lowest temperature of the first desorption at 85 °C, while the one doped with VCl_3 or TiO_2 desorbed at 135 °C and 155 °C, respectively. Interestingly, the temperature of desorption in subsequent cycles of the $NaAlH_4$ doped with TiO_2 reduced to 140 °C. On the contrary, in the case of $NaAlH_4$ doped with $HfCl_4$ or VCl_3, the temperature of desorption increased to 150 °C and 175 °C, respectively. This may be because Ti can disperse in $NaAlH_4$ better than Hf and V; therefore, this affected segregation of the sample after the desorption. The maximum hydrogen absorption capacity can be restored up to 3.5 wt% by doping with TiO_2, while the amount of restored hydrogen was lower for $HfCl_4$ and VCl_3 doped samples. XRD analysis demonstrated that no Ti-compound was observed for the TiO_2 doped samples. In contrast, there was evidence of Al–V alloy in the VCl_3 doped sample and Al–Hf alloy in the $HfCl_4$ doped sample after subsequent desorption/absorption. As a result, the V- or Hf-doped $NaAlH_4$ showed the lower ability to reabsorb hydrogen and required higher temperature in the subsequent desorptions.

Keywords: $NaAlH_4$; TiO_2; VCl_3; $HfCl_4$; Hydrogen desorption/absorption

1. Introduction

Sodium aluminiumhydride or sodium alanate, $NaAlH_4$, has been considered as a candidate media for on-board hydrogen storage in fuel cell applications. One of the advantages of this material is its capability of reversible hydrogen storage [1,2]. This discovery was reported by Bogdanović and Schwickardi [3]. They found that $NaAlH_4$ doped with Ti- or Fe-compound can reabsorb hydrogen at moderate conditions. This ignited the development of complex metal hydrides, particularly $NaAlH_4$ doped with Ti-compound. $NaAlH_4$ has been modified by doping with precious metal catalysts in different forms using different doping techniques [4–10]. However, none has met the U.S. Department of Energy goals (6.0 wt% hydrogen for 2010) [11]. An understanding of the hydrogen desorption/absorption of $NaAlH_4$ doped with transition metal is unclear. The questions are: how do metal dopants activate the hydrogen desorption/reabsorption in $NaAlH_4$; what is the state of metal species after doping; and why does Ti dopant show higher potential than other metal dopants in the hydrogen desorption/reabsorption in $NaAlH_4$? The answers are still not quite understood. There are a number of proposed mechanisms, one of which suggested that Ti dopant might catalyze the hydrogen desorption/absorption of $NaAlH_4$. The substitution of dopant in the lattice of $NaAlH_4$ affects the activation and involves the lattice distortions as proposed by Sun et al. [12]. In the mechanism, Ti is thought to substitute Na^+ and form Ti^{4+} with $Ti(OBu^n)_4$ doped less than 2 mol% resulting in lattice distortions and vacancy formation and enhancement of hydrogen desorption kinetics. However, the proposed mechanisms by Graetz et al. using Ti K-edge X-ray absorption near-edge spectroscopy shows that Ti does not substitute in the bulk lattice nor form Ti metal, but it is present on

* Corresponding author. Tel.: +66 2 218 4135; fax: +66 2 215 4459.
E-mail address: Pramoch.R@chula.ac.th (P. Rangsunvigit).

0378-7753/$ – see front matter © 2006 Elsevier B.V. All rights reserved.
doi:10.1016/j.jpowsour.2006.09.070

the surface in the form of amorphous $TiAl_3$ [13,14]. Recently, Wang et al. directly doped metallic Ti in $NaAlH_4$. They suggested that Ti hydride(s) is in situ formed during the doping process and acts as an active species to catalyze the reversible hydrogen desorption of $NaAlH_4$ [15,16].

The purpose of this work was then to present the effects of a transition metal (TiO_2, VCl_3 and $HfCl_4$) on the hydrogen desorption/reabsorption of $NaAlH_4$ and to understand how each dopant acts in the hydride.

2. Experimental

All experiments in this study were performed under nitrogen atmosphere. The $NaAlH_4$ (90%, Aldrich Chemical) sample was doped with TiO_2 (Degüssa P25), VCl_3 (99%, Merck) or $HfCl_4$ (98%, Aldrich Chemical) using a centrifugal ball mill (Retsch ball mill model S100, stainless steel vial size 250 ml, stainless balls with 1 cm and 2 cm diameters) for 15 min with a speed of 300 rpm. Immediately after mixing, approximately 1 g of a sample was placed into the thermovolumetric apparatus. The high pressure stainless steel reactor (316SS) was heated from room temperature to 280 °C via a furnace controlled by a PID temperature controller. The K-type thermocouple was placed inside the reactor to measure the temperature. The pressure transducer (Cole Parmer, model 68073–68074) was used to measure the pressure change resulting from hydrogen desorption from the sample. For the absorption experiments, hydrogen (99.99%) was used to pressurize the high pressure vessel in a step-wise manner. The sample was reabsorbed at about 120 °C and 10 MPa overnight. Once the pressure reading was constant over a period of time, the data was used to calculate the amount of hydrogen absorbed on the sample. The same procedure was repeated to investigate their reversibility. Samples characterization was also performed using a Rigaku X-ray diffractometer at room temperature over a range of diffraction angles from 28 to 80 with Cu Kα radiation (40 kV, 30 mA) in order to understand the roles of the transition metals on the hydrides.

3. Results and discussion

3.1. Hydrogen desorption/absorption on doped $NaAlH_4$

Fig. 1 shows the temperature program desorption of as-received $NaAlH_4$ doped with 4 mol% TiO_2 (4%TiO_2–$NaAlH_4$). The first step of desorption occurs clearly at 155 °C while the second step takes place at 215 °C with 5.07 wt% hydrogen released. After the desorption, the sample was reabsorbed with hydrogen and desorbed later to determine the amount of reversible hydrogen absorption. We found that the temperature of subsequent desorption decreases about 12 °C and the amount of hydrogen released is 3.4–3.5 wt% hydrogen, as indicated Fig. 1(c). This further confirms that even though their hydrogen absorption capacity and temperature of the subsequent desorption are relatively the same, they are definitely not up to the original sample efficiency.

In the case of hydrogen desorption of $NaAlH_4$ doped with 4 mol% $HfCl_4$ (4%$HfCl_4$–$NaAlH_4$) (Fig. 2) during the first desorption, the sample releases hydrogen at 85 °C and ~150 °C in the subsequent desorption with 5.8 wt% and 2.9–2.45 wt% hydrogen, respectively. This study substantiates that the transition metals increase the desorption/absorption of $NaAlH_4$ and decrease the temperature of desorption compared with the theoretical value (185 °C) [7]. In addition, the reversibility of the sample is not complete and at the point where it starts.

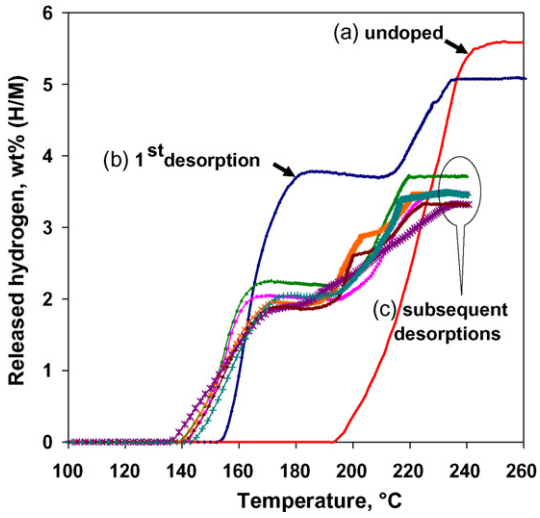

Fig. 1. Correlation between temperature and hydrogen released during hydrogen desorption on $NaAlH_4$ doped with 4 mol% TiO_2 by stainless steel ball milling for 15 min: (a) undoped $NaAlH_4$, (b) first desorption and (c) subsequent desorptions.

The temperature program desorption of $NaAlH_4$ doped with 4 mol% VCl_3 (4%VCl_3–$NaAlH_4$) is shown in Fig. 3. Compared to the $NaAlH_4$ sample doped with TiO_2, the temperatures at which the first and second steps of the first desorption cycle occur about 15–20 °C lower, at 135 °C and 200 °C for the first step and second step, respectively. The amount of hydrogen released, however, is slightly lower, 4.45 wt% hydrogen, because

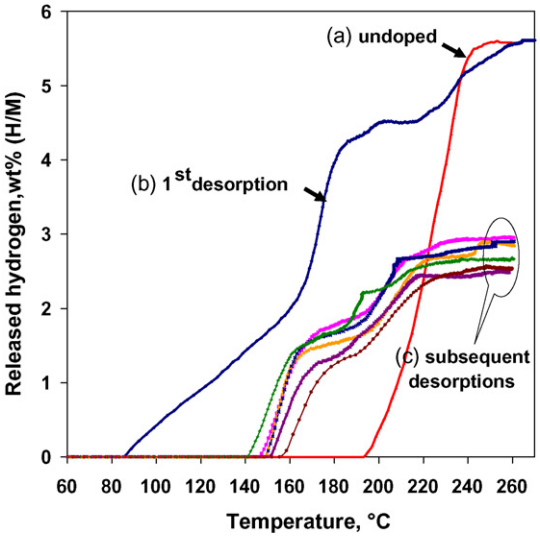

Fig. 2. Correlation between temperature and hydrogen released during hydrogen desorption on $NaAlH_4$ doped with 4 mol% $HfCl_4$ by stainless steel ball milling for 15 min: (a) undoped $NaAlH_4$, (b) first desorption and (c) subsequent desorptions.

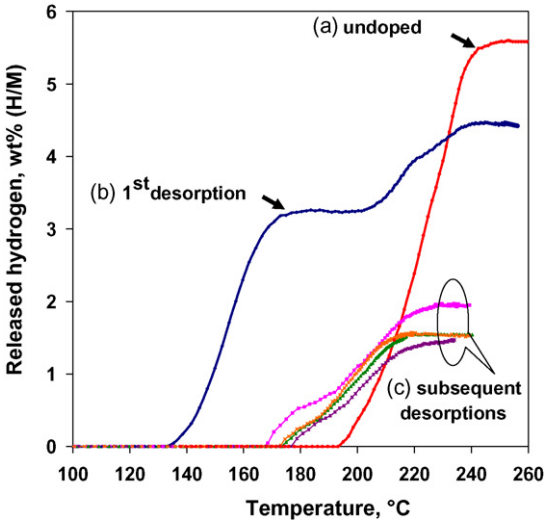

Fig. 3. Correlation between temperature and hydrogen released during hydrogen desorption on $NaAlH_4$ doped with 4 mol% VCl_3 by stainless steel ball milling for 15 min: (a) undoped $NaAlH_4$, (b) first desorption and (c) subsequent desorptions.

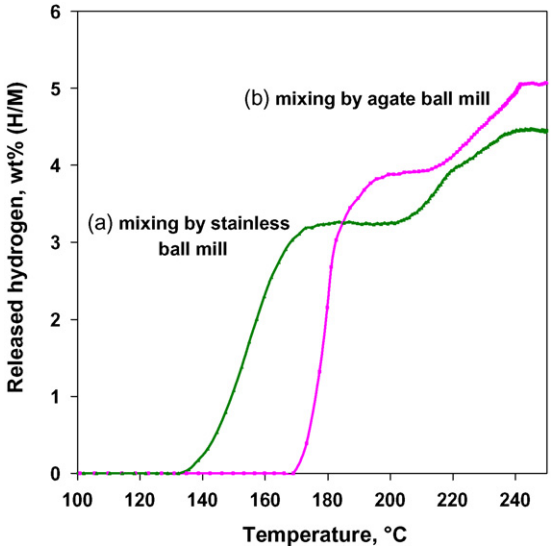

Fig. 4. Correlation between temperature and hydrogen released during hydrogen desorption on $NaAlH_4$ doped 4 mol% VCl_3 by (a) stainless steel ball milling and (b) agate ball milling for 20 min.

some partial decomposition of 4%VCl_3–$NaAlH_4$ occurs during the milling process. For the subsequent desorptions, the amount of released hydrogen drops to 1.5 wt% while the temperature of desorption increases 35 °C from the first desorption cycle. Again, the subsequent absorption experiment results are included in the figure. Clearly, only some fraction of hydrogen storage capability could be attained, and it is less than that of 4%TiO_2–$NaAlH_4$.

Some observations of the effects of different metals on the hydrogen desorption/absorption of $NaAlH_4$ can be made as follows: the decomposition temperature in the first desorption can be compared in the series $HfCl_4 < VCl_3 < TiO_2$. In the case of the decomposition, temperature in the subsequent desorption of 4%TiO_2–$NaAlH_4$ decreases while that doped with $HfCl_4$ and VCl_3 increases as follows: $TiO_2 < HfCl_4 < VCl_3$. Better hydrogen capacity of $NaAlH_4$ doped with TiO_2 than those doped with $HfCl_4$ and VCl_3 can be obtained in the subsequent desorption. It may be suggested that, for the samples loaded with one of these two metals ($HfCl_4$ or VCl_3), it is likely that after the first desorption, the sample particles melt due to the high temperature higher than the melting point of $NaAlH_4$ (178 °C) resulting in the segregation of particles, especially Al particles. This may be attributed to the incomplete subsequent desorption and the need for higher temperature for decomposition in the subsequent cycle. However, for the sample doped with TiO_2, Ti or a Ti-compound may alleviate the segregation of Al and enhance the dispersion in the hydride after the first desorption [1,17]. Although doping TiO_2 shows the highest hydrogen capacity in the subsequent desorption of $NaAlH_4$, the amount of released hydrogen tends to decrease in the subsequent cycle. Haiduc et al. reported that the amorphous Ti–Al tends to form an intermetallic compound at increased temperature during the cycling process. This results in a decrease in the catalytic activity and poor cycling stability [17].

Fig. 4 shows temperature program desorption of 4%VCl_3–$NaAlH_4$ prepared by centrifugal ball milling in different media (stainless steel balls and vial compared with a 250 ml agate vial and five of 1 cm diameter and two of 2 cm diameter agate balls). We found that the sample milled by the stainless ball mill possesses lower desorption temperature than the one milled by agate ball mill, 35 °C. This may be due to the different types of ball mill resulting in different particle sizes, different microstain and homogeneity of the samples. However, the amounts of desorbed hydrogen from both milling media are only slightly different, as indicated by the slopes.

3.2. X-ray diffraction

After hydrogen desorption/absorption, the samples were characterized by the Rigaku X-ray diffractometer. Due to the air sensitivity of the samples, they were covered with a Kapton tape layer to minimize any contamination. To confirm the different particle size of the samples milled by stainless steel balls/vial and the one milled by agate balls/vial, the X-ray line broadening was applied. The X-ray line of the sample milled by stainless steel vial/balls is broader than that of the sample milled by agate vial/balls as shown in Fig. 5. Moreover, we observed that the XRD pattern of the sample milled by stainless steel vial/balls shifts to the lower angle compared with the diffraction peaks of the sample milled by agate vial/balls. This further confirms the difference of particle size and microstrain of the sample milled by stainless steel vial/balls and milled by agate vial/balls that affects the desorption temperature (Fig. 4).

Figs. 6–8 show the XRD patterns of all samples. $NaAlH_4$, NaCl and Al peaks can be observed after the milling for the $HfCl_4$ and VCl_3 doped samples. This result confirms the partial decomposition of the doped hydride during the milling process. On the contrary, only $NaAlH_4$ peaks were observed for the TiO_2 doped sample. No peak of TiO_2 (Fig. 6(b)), $HfCl_4$ (Fig. 7(b)) and VCl_3 (Fig. 8(b)) was observed after milling. Surprisingly, some unknown peaks were clearly found at $2\theta \sim 41°$ in the sam-

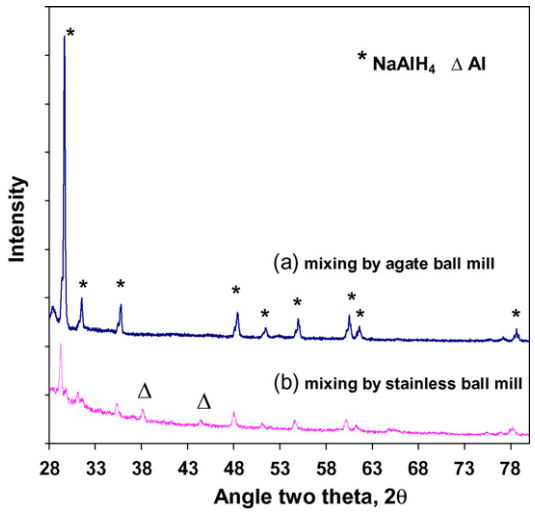

Fig. 5. XRD patterns of $NaAlH_4$ doped 4 mol% VCl_3 by (a) agate ball milling for 20 min and (b) stainless steel ball milling.

ple doped with VCl_3 Fig. 8. The main products after complete decomposition consist of NaH and Al, while the main constituents are $NaAlH_4$ and Al for the reabsorbed hydride doped with TiO_2, $HfCl_4$ and VCl_3. However, by-products in the sample doped with TiO_2 cannot be observed. The increase in the peak intensity and the narrow peak of Al and NaCl show the higher formation of crystallites. Moreover, the intensity of unknown peaks are higher and can be distinctly observed in the VCl_3 doped sample after desorption/reabsorption (Fig. 8(c and d)). These peaks were expected to be the formation of V-species. Peak identification using JCPD-International Centre for Diffraction Data suggested that they should be peaks of an intermetallic compound of V–Al in the form of Al_3V. This supports the visibility of V–Al peaks in VCl_3 doped $NaAlH_4$. In addition, no peak is observed in $HfCl_4$ or TiO_2 doped $NaAlH_4$. To determine the form of the Hf-compound in the $NaAlH_4$ sample, 10 mol% $HfCl_4$ were doped in $NaAlH_4$, after the subsequent hydrogen desorption/absorption, the sample doped with 10%$HfCl_4$ was dissolved in THF (>99.998%, J.T. Baker), stirred for 2 h and centrifuged in order to separate the precipitate. Finally, the

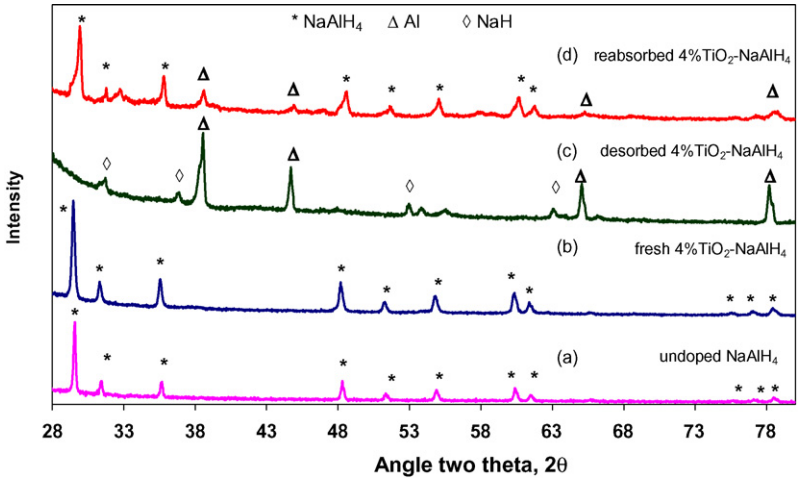

Fig. 6. XRD patterns of (a) as-received $NaAlH_4$, (b) 4%TiO_2–$NaAlH_4$, (c) 4%TiO_2–$NaAlH_4$ after subsequent desorption and (d) 4%TiO_2–$NaAlH_4$ after reabsorption.

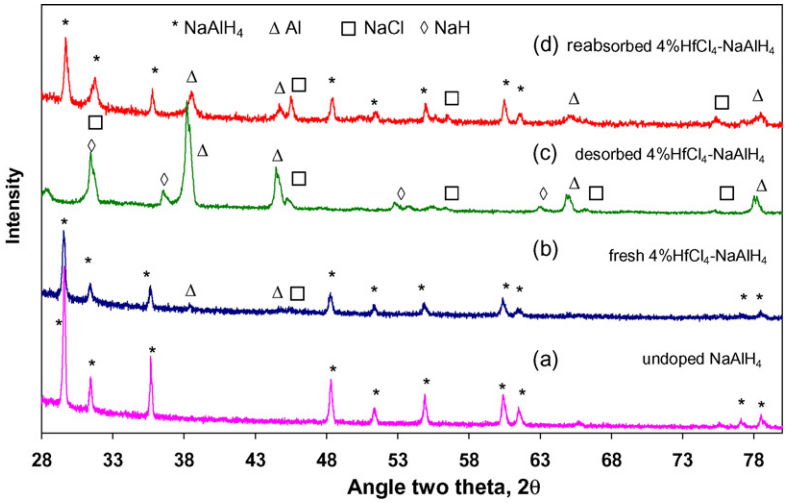

Fig. 7. XRD patterns of (a) as-received $NaAlH_4$, (b) 4%$HfCl_4$–$NaAlH_4$, (c) 4%$HfCl_4$–$NaAlH_4$ after subsequent desorption and (d) 4%$HfCl_4$–$NaAlH_4$ after reabsorption.

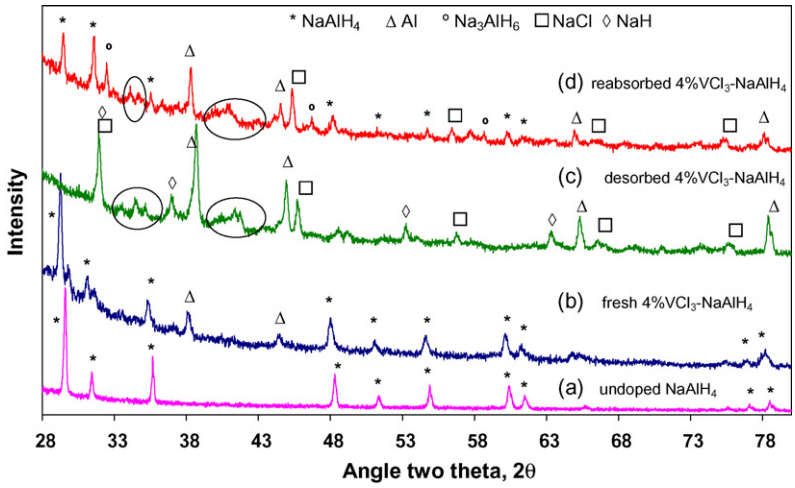

Fig. 8. XRD patterns of (a) as-received $NaAlH_4$, (b) 4%VCl_3–$NaAlH_4$, (c) 4%VCl_3–$NaAlH_4$ after subsequent desorption and (d) 4%VCl_3–$NaAlH_4$ after reabsorption.

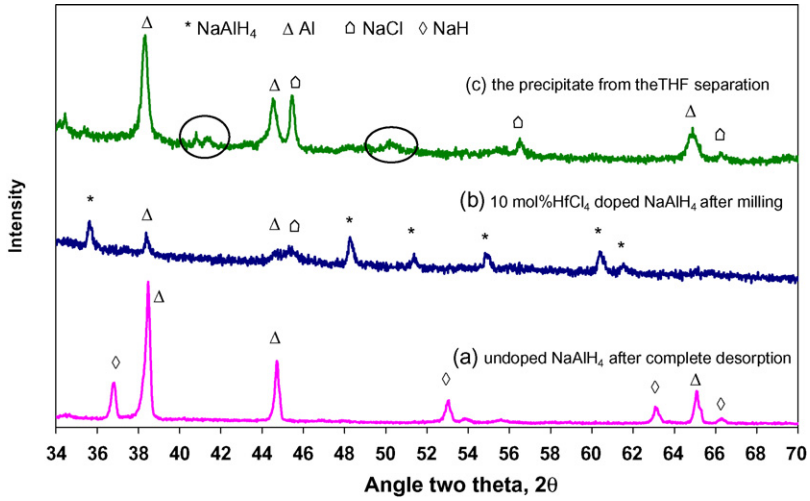

Fig. 9. XRD patterns of (a) undoped $NaAlH_4$ after complete desorption, (b) 10%$HfCl_4$–$NaAlH_4$ after milling and (c) the precipitate from THF solution.

precipitate was dried by vacuum and characterized by XRD. Surprisingly, the XRD pattern of the THF precipitated sample shows some unknown peaks at $2\theta \approx 41.5^\circ$ and 50.48°, which match with the reference data base of intermetallic compound between Al–Hf would be in form of Al_3Hf as shown in Fig. 9(c).

The above results are suggested that Ti lacks the long-range order to form Ti–Al crystal structure and would form as Ti–Al amorphous or be very dispersed particle on $NaAlH_4$, which evidences by XRD as suggested by Graetz et al. [13] and Weidenthaler et al. [18], while V or Hf shows the strong formation of V–Al or Hf–Al crystalline. As the result, the V- or Hf-doped $NaAlH_4$ shows a lower ability to reabsorb hydrogen than that doped with Ti. The formation of Al_3V or Al_3Hf intermetallic is a stable compound that would decrease the activity of the catalyst. In other words, the high stability of Al_3V or Al_3Hf would affect the reformation to $NaAlH_4$. In addition, the formation of crystal Al_3V or crystal Al_3Hf would reduce the amount of Al metallic to reabsorb hydrogen. Moreover, the formation of intermetallic compound between Al with Hf or V would separate the transition metal from the hydride after the high temperature desorption that causes the subsequent desorption behaviour shifted to be closer to that of the undoped hydride (Figs. 2 and 3). For the Ti-doped hydride, it seems that the formation of the unstable Ti–Al amorphous promotes the reduction of Al metallic to hydride, compared with those of the undoped and V- or Hf-doped hydrides. Comparisons among the intensity of $NaAlH_4$ to Al ratio in the XRD results of $NaAlH_4$ doped with TiO_2 (Fig. 6(d)), $HfCl_4$ (Fig. 7(d)) and VCl_3 (Fig. 8(d)) after the hydrogen reabsorption show that the TiO_2 doped sample demonstrates the highest intensity of $NaAlH_4$ to Al ratio. This indicates that more Al in the sample doped with TiO_2 is converted to $NaAlH_4$ than that doped with $HfCl_4$ or VCl_3 as previously discussed.

4. Conclusion

Doping transition metals (TiO_2, $HfCl_4$, or VCl_3) on $NaAlH_4$ affects the hydrogen desorption/absorption. Ti doping seems to be the most effective dopant among the three tested transition metals. By doping the hydride with TiO_2, the maximum hydrogen absorption capacity can be restored at 3.5 wt%. That may be attributed to the formation of Ti–Al amorphous that can be

reduced to the hydride easily and prevent the segregation of metallic Al. In contrast, V or Hf prefers to the form order of Al_3V or Al_3Hf, which would decrease the activity of the catalyst in the hydrogen desorption/reabsorption. Using different milling media (stainless steel media and agate media) also results in different hydrogen desorption behaviours.

Acknowledgements

This work was supported by the National Science and Technology Development Agency (Reverse Brain Drain Project), the Petroleum and Petrochemical College (PPC), the Research Unit for Petrochemical and Environment Catalysts, the Ratchadapisek Somphot Endowment, and The Petroleum and Petrochemical Technology Consortium, Chulalongkorn University; and UOP LLC.

References

[1] C.M. Jensen, K.J. Gross, Appl. Phys. A 72 (2001) 213–219.
[2] E. Fakioğlu, Y. Yűrűm, T.N. Veziroğlu, Int. J. Hydrogen Energy 29 (2004) 1371–1376.
[3] B. Bogdanović, M. Schwickardi, J. Alloys Compd. 253–254 (1997) 1–9.
[4] A. Zidan, S. Takara, A. Hee, C.M. Jensen, J. Alloys Compd. 285 (1999) 119–122.
[5] M. Jensen, R. Zidan, N. Mariels, A. Hee, C. Hagen, Int. J. Hydrogen Energy 24 (1999) 461–465.
[6] C.M. Jensen, S. Takara, Proceedings of the 2000 on Hydrogen Program Review NREL/CP-570-28890, 2000.
[7] B. Bogdanović, R.A. Brand, A. Marjanovic, M. Schwickardi, J. Tolle, J. Alloys Compd. 302 (2000) 36–58.
[8] K.J. Gross, E.H. Majzoub, S.W. Spangler, J. Alloys Compd. 356–357 (2003) 423–428.
[9] G. Sandrock, K. Gross, G. Thomas, J. Alloys Compd. 399 (2002) 299–308.
[10] D.L. Anton, J. Alloys Compd. 356–357 (2003) 400–404.
[11] D. Sun, S. Ma, Y. Ke, D.J. Collins, H.C. Zhou, J. Am. Chem. Soc. 128 (2006) 3896–3897.
[12] D. Sun, T. Kiyobayashi, H.T. Takeshita, N. Kuriyama, C.M. Jensen, J. Alloys Compd. 337 (2002) L8–L11.
[13] J. Graetz, J.J. Reilly, Johnson, J. Appl. Phy. Lett. 85 (2004) 500–503.
[14] H.W. Brink, C.M. Jensen, S.S. Srinivasan, B.C. Hauback, D. Blanchard, K. Murphy, J. Alloys Compd. 376 (2004) 215–221.
[15] P. Wang, C.M. Jensen, J. Alloys Compd. 379 (2004) 99–102.
[16] P. Wang, X.D. Kang, H.M. Cheng, J. Phys. Chem. B 109 (2005) 20131–20136.
[17] A.G. Haiduc, H.A. Stil, M.A. Schwarz, P. Paulus, J.J.C. Geerlings, J. Alloys Compd. 393 (2005) 252–263.
[18] C. Weidenthaler, A. Pommerin, M. Felderhoff, B. Bogdanović, F. Schuth, Phys. Chem. Chem. Phys. 5 (2003) 5149–5153.